

Supporting Information

Whitney et al. 10.1073/pnas.1420536112

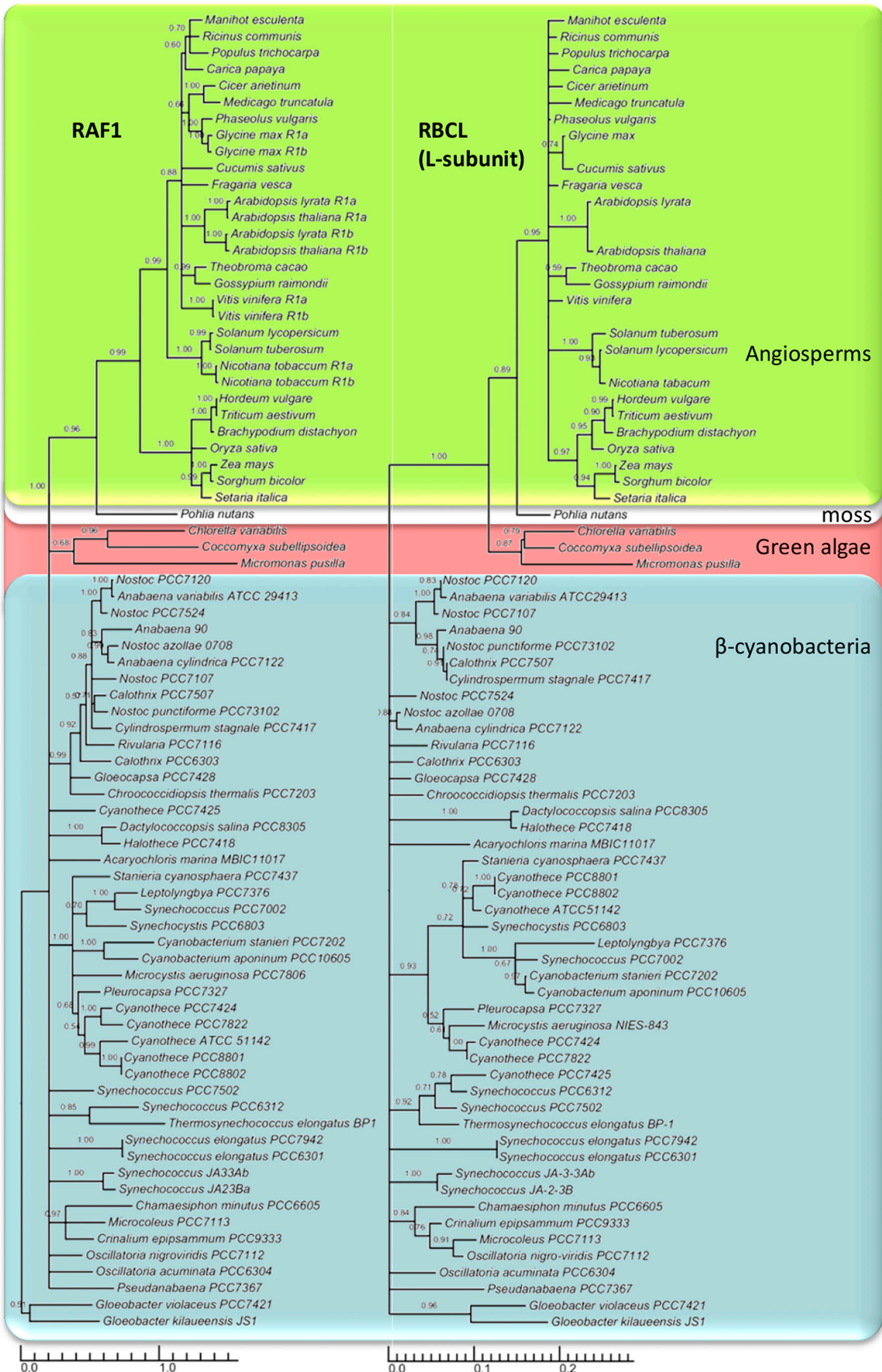
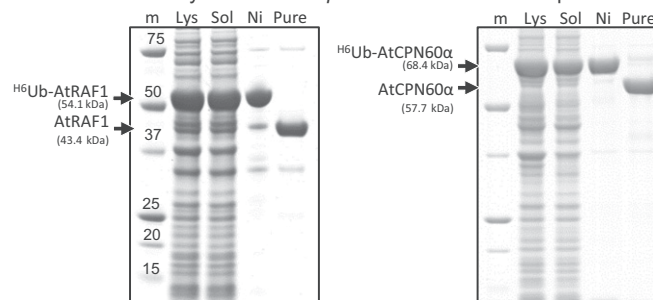


Fig. S1. RAF1 and Rubisco L-subunits phylogenies of plants, green algae, and β -cyanobacteria. (A) Maximum-likelihood trees assembled under the Dayhoff model implemented in RAxML v.8 (1) using translated amino acid sequences from the full length *raf1* and *rbcl* genes listed in Table S2. Posterior probability (PP) values are shown above tree branches; all clades with PP < 0.5 have been dissolved.

1. Stamatakis A (2014) RAxML version 8: A tool for phylogenetic analysis and post-analysis of large phylogenies. *Bioinformatics* 30(9):1312–1313.

A SDS PAGE analysis of *Arabidopsis* RAF1 and CPN60 α purification



B SDS PAGE immuno-blot quantification of leaf AtRAF1 expression

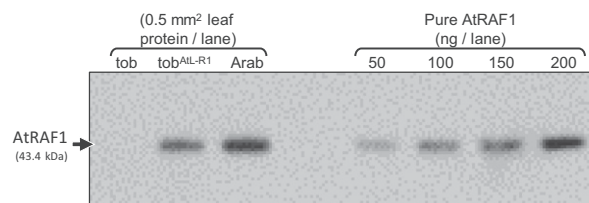


Fig. S3. CPN60 α and ^ARAF1 purification and quantification by immunoblot analysis. The mature coding sequence CPN60 α 1 (GenBank NP_197383.1, At5g18820) from *Arabidopsis* (i.e., spanning amino acids 36–578 to exclude part or all of the chloroplast targeting sequence) was amplified by RT-PCR (SuperScript III Reverse Transcriptase, Life Technologies) using leaf RNA extracted using TRIzol Reagent (Life Technologies) and primers 5'SacIIAtCPN60 α (5'-CCGCGGTGGAATGGGAGCTAAGAGAATACTATAC-3') and 3'HindIII AtCPN60 α (5'-AAGCTTATGATGTGGGTATGCCAGG-3'). The amplified 1637-bp SacII-HindIII product was cloned in frame with the N-terminal 6x-histidine (H_6)-Ub fusion peptide in plasmid pHue (1) to give plasmid pHueCPN60 α . Similarly, the synthetic ^Araf1 gene in pLEVAtL-RAF1 (Fig. 2A) was amplified with primers 5'SacIIAtRAF1 (5'-CCGCGGTGGAATGGCTCCTTAAATCTTTGATT-3') and 3'HindIIIAtRAF1 (5'-AAGCTTCTCGAGATCCCAATTTTGATG-3') and the 1,364-bp SacII-HindIII fragment cloned into pHue to give pHueAtRAF1. *Escherichia coli* BL21 (DE3) cells transformed with plasmids pHueAtRAF1 and pHueCPN60 α were grown at 28 °C on a rotary shaker (150 rpm) in 0.5 L of Luria-Bertani medium containing 200 μ g/mL ampicillin. At an A_{600} of 1.0 isopropyl- β -D-thiogalactopyranoside was added to 0.5 mM. After 6 h, the cells were harvested by centrifugation ($3,300 \times g$, 10 min, 4 °C) and resuspended in 10 mL of ice-cold extraction buffer (0.1 M Tris-HCl, pH 8.0, 0.3 M NaCl, 1 mM PMSF, 5 mM mercaptoethanol) and lysed by passage through a prechilled French pressure cell at 140 MPa. The extract was centrifuged ($33,000 \times g$, 10 min, 4 °C) and the (H_6)-Ub-RAF1 and (H_6)-UbCPN60 α proteins purified by Ni²⁺-nitrilotriacetic acid (Ni-NTA) agarose (Qiagen) chromatography, eluted in imidazole buffer (extraction buffer with 0.2M imidazole) and the (H_6)-Ub sequences removed with a (H_6)-Ub-protease as described (1) before dialyzing into storage buffer [40 mM EPPS-NaOH, pH8, 8 mM MgCl₂, 0.8 mM EDTA, 20% (vol/vol) glycerol] and storing at -80 °C. (A) Protein samples during the purification were diluted with 0.25-volumes 4 \times SDS reducing buffer and analyzed by SDS PAGE as described previously (2). (B) The ^ARAF1 content in soluble protein from known leaf areas were calculated by immuno-blot densitometry analysis against known amounts of purified ^ARAF1 (quantified against BSA standards) separated in parallel by SDS PAGE.

1. Baker RT, et al. (2005) Using deubiquitylating enzymes as research tools. *Methods Enzymol* 398:540–554.

2. Whitney SM, Sharwood RE (2007) Linked Rubisco subunits can assemble into functional oligomers without impeding catalytic performance. *J Biol Chem* 282(6):3809–3818.

PAGE analysis of leaf soluble and NiNTA purified protein

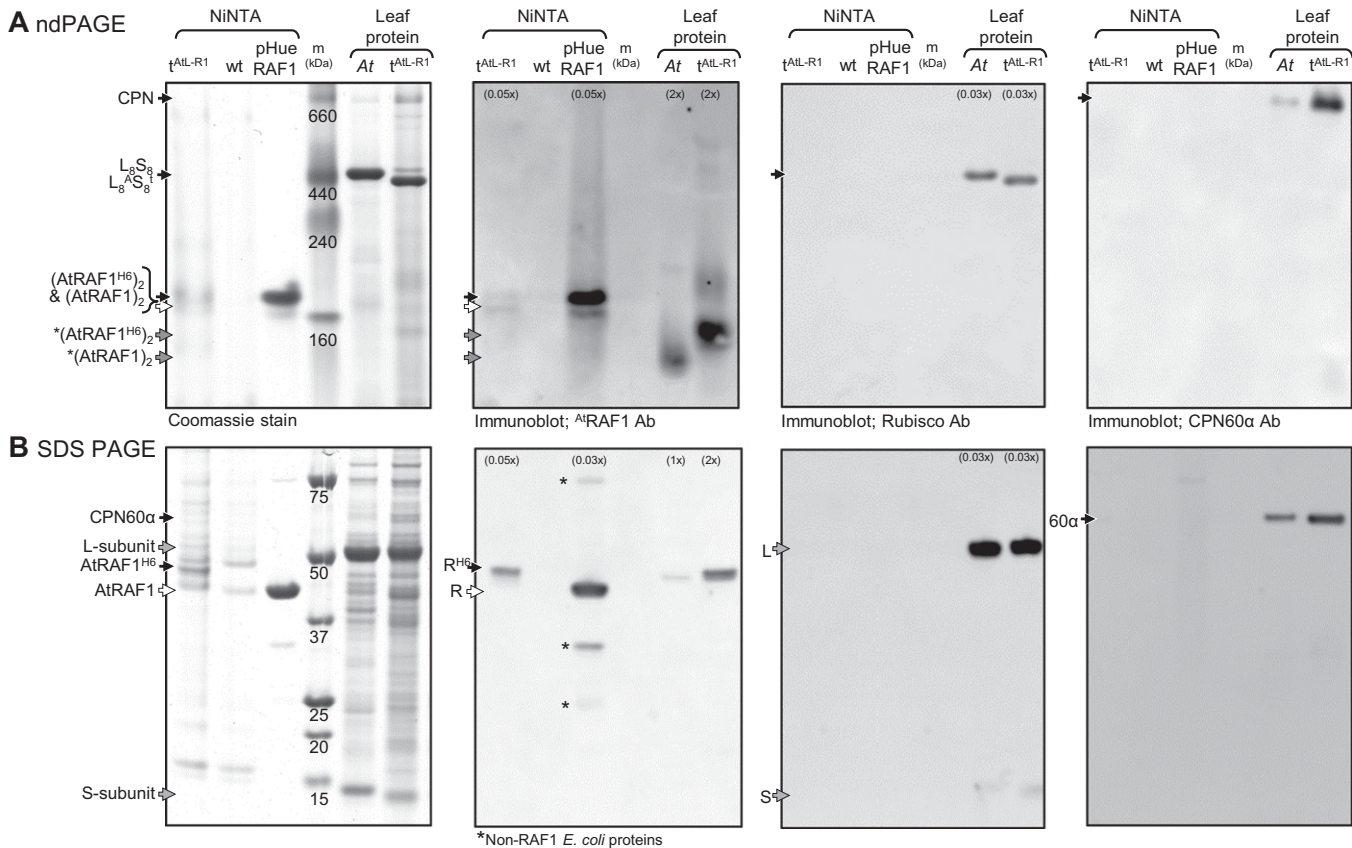
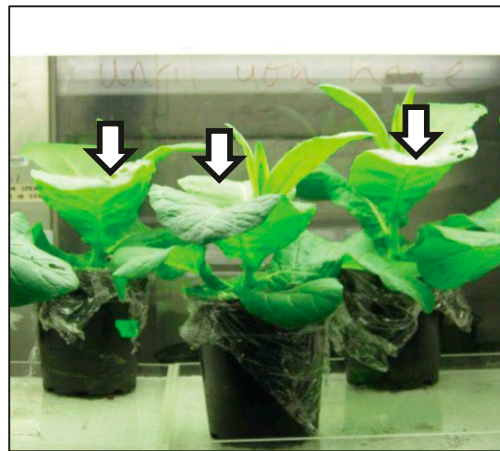


Fig. 54. PAGE analysis of NiNTA purified and total soluble leaf protein from *Arabidopsis* and the different tobacco genotypes. (A) ndPAGE and (B) SDS PAGE analysis of soluble leaf protein [from *Arabidopsis* (At), *tob*^{AtL-R1} and *tob*^{AtL}] and Ni²⁺-nitrilotriacetic acid agarose (Ni-NTA) purified protein from *E. coli*-pHueAtRAF1 cells (Fig. S3), tobacco (wild-type) and *tob*^{AtL-R1} leaves. Variations in the amount of sample loaded per lane relative to the Coomassie-stained gel are shown in parentheses. For NiNTA purification ~2 g of *tob*^{AtL-R1} and wild-type tobacco leaves were homogenized in 20 mL extraction buffer [0.1 M Tris-HCl, pH 8.0, 0.3 M NaCl, 5% (vol/vol) glycerol, 1% (wt/vol) PVPP, 1 mM PMSF, 5 mM mercaptoethanol] using 40 mL Wheaton glass homogenizers, then centrifuged (16,500 × g, 10 min, 2 °C). The soluble protein was transferred to a 10-mL Econo column (Promega) containing a 1-mL bed volume of Ni-NTA agarose (Qiagen). After the sample had passed through the resin, it was washed with 20 bed volumes of extraction buffer (no PVPP or mercaptoethanol). The bound protein was collected in 0.8 mL of elution buffer (0.1 M Tris-HCl, pH 8.0, 0.3 M NaCl, and 200 mM imidazole) and the proteins separated by PAGE, as described previously (1). Immunoblot analysis confirmed the ^{At}RAF1 purified from *tob*^{AtL-R1} comprised two similar sized bands that matched the size of those purified from *E. coli*. In the At and *tob*^{AtL-R1} soluble leaf protein samples the native ^{At}RAF1 and slightly larger recombinant ^{At}RAF1^{H6} products are seen as more diffuse bands of lower apparent molecular size. No Rubisco or CPN60α subunits were detected in the NiNTA purified protein from *tob*^{AtL-R1} or wild-type. Only the ^{At}RAF1 protein was visually unique in the Coomassie-stained NiNTA purified protein from *tob*^{AtL-R1} suggesting it does not stably interact with any other tobacco chloroplast protein to any significant extent, although this requires closer proteomic scrutiny.

1. Whitney SM, Sharwood RE (2007) Linked Rubisco subunits can assemble into functional oligomers without impeding catalytic performance. *J Biol Chem* 282(6):3809–3818.

A Plant phenotype and experimental setup for analyzing Rubisco synthesis and turnover in whole leaves by ^{35}S -Met pulse-chase



B Schematic of the leaf pulse-chase analysis abaxial infiltration and sampling régime

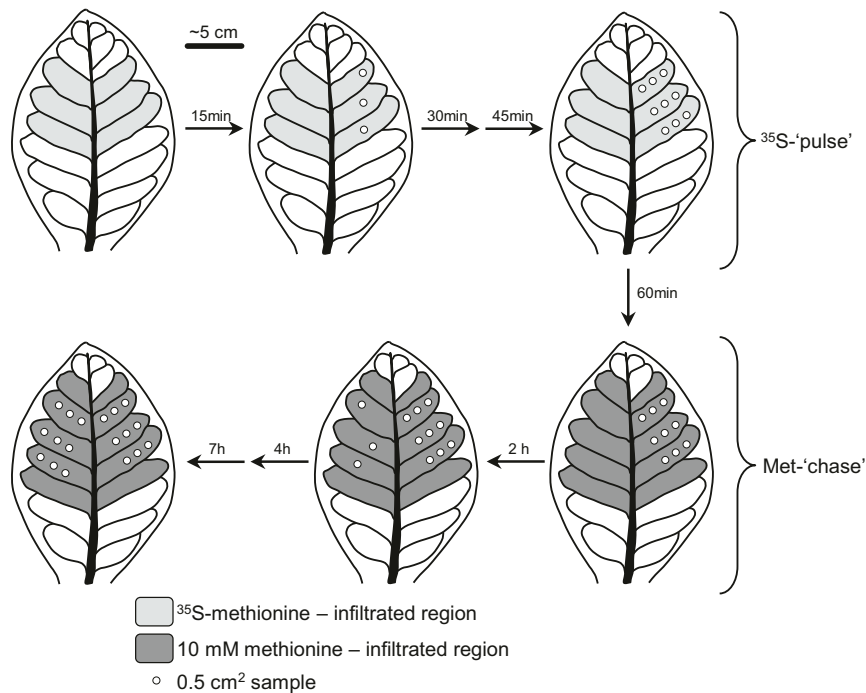


Fig. S5. ^{35}S -labeling of Rubisco in attached tobacco leaves by a direct infiltration approach. Because of significant variations in Rubisco expression down the canopy of tobacco (1), significant care was taken to perform the ^{35}S -infiltration experiments on leaves of comparable developmental status and positioning in the upper canopy. (A) The plants analyzed were all of comparable size with infiltration experiments performed on the youngest near fully expanded leaf (the fifth from the top of the canopy, indicated by white arrow) where the intercellular air spaces are optimally developed for fast and efficient liquid infiltration. (B) Showing the regions of the leaves toward the tip that were infiltrated in the experiment and the sampling protocol undertaken during both the [^{35}S]methionine labeling ('pulse') and ensuing 10-mM methionine "chase" period.

1. Pengelly JJ, et al. (2014) Transplastomic integration of a cyanobacterial bicarbonate transporter into tobacco chloroplasts. *J Exp Bot* 65(12):3071–3080.

Table S1. Rubisco catalysis comparison

Plant source	Tobacco	<i>Arabidopsis</i>	tob ^{Atl-R1}
k_C^{cat} (s ⁻¹)	3.1 ± 0.1	3.0 ± 0.2	2.3 ± 0.3*
K_C (μM)	9.7 ± 0.2	9.8 ± 0.3	8.6 ± 0.2*
K_O (μM)	174 ± 16	192 ± 17	221 ± 16
$k_C^{cat}/K_C^{21\%O_2}$ (mM ⁻¹ /s ⁻¹)	138	125	126
S_{CO} (mol/mol ⁻¹)	82 ± 1	80 ± 2	80 ± 3

*Significance variation ($P < 0.05$) determined by t -test. $K_C^{21\%O_2}$, the apparent K_m for CO₂ (K_C) at atmospheric [O₂] (assumed 252 μM at 25 °C) calculated as $K_C(1+[O_2]/K_O)$.

Table S2. List of species and accession numbers for the *raf1* and *rbcl* sequences from 26 plant, 3 algal, and 46 cyanobacteria genomes used to construct the maximum-likelihood trees in Fig. S1

Organism	<i>raf1</i>	<i>rbcl</i>	<i>matK</i>
Angiosperms			
<i>Arabidopsis lyrata</i>	XM_002882316; XM_002872267	XM_002888303	AF144342
<i>Arabidopsis thaliana</i>	BT015787; AY063107	U91966ATU91966	AF144378
<i>Brachypodium distachyon</i>	XM_003573939	194033128:54293–55723	133917479
<i>Carica papaya</i>	Phytozome: 162.24_CDS	EU431223:58728–60155	EU431223:2266–3786
<i>Cicer arietinum</i>	XM_004495508	197294093:5003–6430	197294093:2070–3599
<i>Cucumis sativus</i>	XM_004142526	DQ865976:57578–59005	68164782:1838–3376
<i>Fragaria vesca</i>	XM_004304718	325126844:56459–57886	AF288102
<i>Glycine max</i>	XM_003536095; XR137658	91214122:5312–6739	AF142700
<i>Gossypium raimondii</i>	Phytozome:013G120100.1_CDS	372290914:58642–60081	AF403559
<i>Hordeum vulgare</i>	AK353664	AY137453:111–1550	AB078139
<i>Manihot esculenta</i>	Phytozome:03614:2579552.0.2581338	169794052:58063–59496	EU117376:2063–3583
<i>Medicago truncatula</i>	BT141443	JX512024:117295–118722	AY386945
<i>Nicotiana tobaccum</i>	current study	NC_001879	81238323:2131–3660
<i>Oryza sativa</i>	115482237	AY522330:54082–55536	EU434287
<i>Phaseolus vulgaris</i>	KF033821	EU196765:70304–71734	AY582987
<i>Populus trichocarpa</i>	XM_002319615	134093177:55716–57143	134093177:1981–3513
<i>Ricinus communis</i>	XM_002521916	372450118:58961–60388	372450118:2387–3907
<i>Setaria italica</i>	XM_004982939	558603649:54628–56034	390607728
<i>Solanum lycopersicum</i>	XM004249865	544163592:56683–58116	544163592:2124–3653
<i>Solanum tuberosum</i>	565368659	DQ386163.2:56531–57964	JF772171:2140–3669
<i>Sorghum bicolor</i>	XM_002448739	118614470:57693–59123	AF164418
<i>Theobroma cacao</i>	Phytozome: EG026242t1_CDS	JQ228389:59398–60852	AY321195
<i>Triticum aestivum</i>	AK334642	AY328025:60–1493	KJ592713:1678–3216
<i>Vitis vinifera</i>	FQ395584; FQ393164	91983971:59436–60863	91983971:2016–3524
<i>Zea mays</i>	226508017	11994090:56874–58304	11994090:1674–3215
Bryophyta			
<i>Pohlia nutans</i>		AY631193	AY522574
Green Algae			
<i>Coccomyxa subellipsoidea</i>	XM_005643171	HQ693844:164006–165433	323149147:70601–72805
<i>Chlorella variabilis</i>	XM_005847023	331268093:47431–48858	331268093:26130–28334
<i>Micromonas pusilla</i>	XM_003063100	FJ858267:20006–21433	FJ858269
β-Cyanobacteria			
<i>Acaryochloris marina MBIC11017</i>	CP000828:1771175–1772245	CP000828:1775408–1776838	
<i>Anabaena cylindrica PCC 7122</i>	CP003659:5732014–5733099	CP003659:34579–36009	
<i>Anabaena sp 90</i>	CP003284:2564028–2565113	CP003284:1480330–1481760	
<i>Anabaena variabilis ATCC 29413</i>	CP000117:1756144–1757229	CP000117:4857469–4858899	
<i>Calothrix sp PCC 6303</i>	CP003610:4364743–4365828	CP003610:3605242–3606672	
<i>Calothrix sp PCC 7507</i>	CP003943:5400132–5401217	CP003943:325257–326687	
<i>Chamaesiphon minutus PCC 6605</i>	CP003600:6052812–6053882	CP003600:694685–696115	
<i>Chroococcidiopsis thermalis PCC 7203</i>	CP003597:1959990–1961051	CP003597:5964292–5965722	
<i>Crinalium epipsammum PCC 9333</i>	CP003620:4318634–4319728	CP003620:4709290–4710720	
<i>Cyanobacterium aponinum PCC 10605</i>	CP003947:3620023–3621099	CP003947:800936–802342	
<i>Cyanobacterium stanieri PCC 7202</i>	CP003940:251659–252741	CP003940:126365–127771	
<i>Cyanothece sp ATCC 51142</i>	CP000806:1951795–1952787	CP000806:3281510–3282925	
<i>Cyanothece sp PCC 7424</i>	CP001291:3045110–3046189	CP001291:1503225–1504643	
<i>Cyanothece sp PCC 7425</i>	CP001344:4048780–4049862	CP001344:3372918–3374348	
<i>Cyanothece sp PCC 7822</i>	CP002198:3872031–3873092	CP002198:3223935–3225353	
<i>Cyanothece sp PCC 8801</i>	CP001287:819957–821021	CP001287:1677472–1678890	
<i>Cyanothece sp PCC 8802</i>	CP001701:819755–820819	CP001701:1666285–1667703	
<i>Cylindrospermum stagnale PCC 7417</i>	CP003642:6936516–6937604	CP003642:2391125–2392555	
<i>Dactylococcopsis salina PCC 8305</i>	CP003944:2505154–2506221	CP003944:1798755–1800176	
<i>Gloeobacter kilaeensis JS1</i>	CP003587:711901–712965	CP003587:713821–715245	
<i>Gloeobacter violaceus PCC 7421</i>	37508091:2309302–2310369	37508091:2307046–2308470	
<i>Gloeocapsa sp PCC 7428</i>	CP003646:1785908–1786993	CP003646:1141494–1142924	
<i>Halotheca sp PCC 7418</i>	CP003945:2360587–2361660	CP003945:3829408–3830826	
<i>Leptolyngbya sp PCC 7376</i>	CP003946:2022725–2023804	CP003946:204758–206173	
<i>Microcoleus sp PCC 7113</i>	CP003630:771030–772124	CP003630:2675003–2676433	
<i>Microcystis aeruginosa PCC 7806</i>	159027328:13224–14216	166085114:4390428–4391843	
<i>Nostoc azollae 708</i>	CP002059:4390613–4391698	CP002059:2235547–2236977	
<i>Nostoc punctiforme PCC 73102</i>	CP001037:5521656–5522744	CP001037:5263600–5265030	
<i>Nostoc sp PCC 7107</i>	CP003548:2972009–2973094	CP003548:2119530–2120960	

Table S2. Cont.

Organism	<i>raf1</i>	<i>rbcl</i>	<i>matK</i>
<i>Nostoc sp PCC 7120</i>	47118302:6264560–6265645	47118302:1785970–1787400	
<i>Nostoc sp PCC 7524</i>	CP003552:4087403–4088488	CP003552:1290272–1291702	
<i>Oscillatoria acuminata PCC 6304</i>	CP003607:7273598–7274692	CP003607:1163939–1165369	
<i>Oscillatoria nigro-viridis PCC 7112</i>	CP003614:6651808–6652902	CP003614:6951541–6952971	
<i>Pleurocapsa sp PCC 7327</i>	CP003590:3516618–3517697	CP003590:357448–358863	
<i>Pseudanabaena sp PCC 7367</i>	CP003592:182052–183158	CP003592:1184484–1185896	
<i>Rivularia sp PCC 7116</i>	CP003549:6792297–6793388	CP003549:4304946–4306376	
<i>Stanieria cyanosphaera PCC 7437</i>	CP003653:1606913–1607992	CP003653:369045–370463	
<i>Synechococcus elongatus PCC 6301</i>	56684969:792692–793771	56684969:139920–141338	
<i>Synechococcus elongatus PCC 7942</i>	CP000100:827112–828182	CP000100:1479461–1480879	
<i>Synechococcus sp JA-2-3Ba(2-13)</i>	CP000240:535600–536703	CP000240:2682338–2683762	
<i>Synechococcus sp JA-3-3Ab</i>	CP000239:929252–930337	CP000239:1207204–1208628	
<i>Synechococcus sp PCC 6312</i>	CP003558:1545379–1546446	CP003558:1977136–1978563	
<i>Synechococcus sp PCC 7002</i>	CP000951:2467879–2468958	CP000951:1882749–1884164	

Two gene copies of *raf1* were found in five plant species (including tobacco and *Arabidopsis*; see Fig. S2B), and one copy in all other species. Accession numbers are also shown for the chloroplast *matK* sequences that were used as a negative control when testing for putative *raf1* and *rbcl* coevolution by correlating their pairwise nonsynonymous (leading to amino acid substitutions) and synonymous (selectively neutral) distances across green plants and algae (see Fig. 1B).